ARTICLES

Metal-insulator transition in oriented poly(*p*-phenylenevinylene)

M. Ahlskog, Reghu Menon, and A. J. Heeger
Institute for Polymers and Organic Solids, University of California at Santa Barbara, Santa Barbara, California 93106

T. Noguchi and T. Ohnishi
Sumitomo Chemical Co. Ltd., Tsukuba Research Laboratory, 6 Kitahara, Tsukuba, Ibaraki, 300-32, Japan
(Received 23 May 1996)

The transport properties of H_2SO_4-doped, tensile drawn, and oriented poly(phenylenevinylene) have been studied in the metallic, critical, and insulating regimes of the disorder-induced metal-insulator transition (M-I) transition. The temperature dependence of the conductivity, $\sigma(T)$ and the magnetoconductance (MC) were investigated between room temperature and 1.3 K and in magnetic fields up to 8 T, in freshly doped samples and in samples during controlled dedoping (aging). A complete set of measurements were carried out on a single, fully doped sample that was followed during ageing from the metallic state through the critical regime into the insulting state. The transport properties are characterized as a function of the resistivity ratio (ρ_r), where $\rho_r=[\rho(1.3\ \mathrm{K})/\rho(200\ \mathrm{K})]$. In the metallic regime ($\rho_r<2$), $\sigma_{\parallel}$ (300 K)$\cong$10 000 S/cm and $\sigma_{\perp}$ (300 K)$\cong$100 S/cm; for $T<4$ K, a $T^{1/2}$ dependence is observed for $\sigma(T)$, and the MC shows positive and negative contributions at low and high fields, respectively. The positive contribution to the MC vanishes at the M-I transition boundary ($\rho_r\cong 2$). The behaviors of $\sigma(T)$and the MC are consistent with the weak localization plus electron-electron interaction model. Very near the M-I transition, a field-induced transition from the metallic to the critical regime was observed $\{\sigma(T)\propto T^{0.1}$ at 8 $T\}$. For samples in the critical regime with $4<\rho_r<30$, $\sigma(T)\propto T^{\beta}$ at low temperatures. In the insulating state ($\rho_r>50$), $\rho(T)\propto\exp(T_0/T)^x$ indicating variable-range-hopping transport. Although anisotropic, the field and temperature dependences of the transport are similar both parallel and perpendicular to the chain axis, implying that oriented conducting polymers are anisotropic three-dimensional conductors. [S0163-1829(97)07611-X]

I. INTRODUCTION

Recent improvements in the quality of doped conducting polymers have enabled a clear demonstration of the achievement of the metallic state with the Fermi level in an energy interval in which the electronic wave functions are delocalized.[1] The fundamental fact that several doped conducting polymer systems, including polyacetylene $(CH)_x$, poly(*p*-phenylenevinylene) (PPV), polyaniline, and polypyrrole (PPy), have a large finite conductivity as the temperature approaches zero indicates that the metallic state is intrinsic to these systems. The absence of long-range structural order in these disordered polymers strongly affects the electronic transport properties in the metallic state, as can be seen in the negative temperature coefficient of resistivity (TCR). Thus doped conducting polymers are characterized as disordered metals near the boundary of the disorder-induced metal-insulator (M-I) transition.

From previous work on doped conducting polymers, it is known that disorder causes the M-I transition. A fundamental issue is whether these systems should be viewed as homogeneous or whether relatively large scale inhomogeneities are involved (a granular metal made up of ''metallic islands'').[1(b)] If the localization length and/or correlation length near the M-I transition are larger than the crystalline coherence length, then the disorder can be considered as homogeneous for the interpretation of the transport data. Conversely, in the localization length and/or correlation length are smaller than the crystalline coherence length, then the system behaves more like a granular metal. In the former case, the M-I transition can be viewed in the context of disorder-induced localization. In the latter case, the M-I transition would be better characterized as a connectivity-induced percolation transition. Detailed analysis of the transport data have shown that all aspects of the transport data are in agreement with disorder-induced localization as the mechanism of the M-I transition. Moreover, the observation of Mott's $\ln\sigma\propto T^{-1/2}$ dependence of conductivity at low temperatures on the insulating side of M-I transition implies that the disorder potentials are within the homogeneous limit even in this regime. The $\ln\sigma\propto T^{-1/2}$ dependence characteristic of granular metals is observed only deep in the insulating regime or in blends with insulating polymers at concentrations below the percolation threshold.[1]

Because of the intrinsic quasi-one-dimensional (quasi-1D) character of the electronic structure of conducting polymers, it is of interest to compare the disorder-induced M-I transition in these systems and in three-dimensional systems. For example, the power-law dependence of resistivity $[\rho(T)\propto T^{\beta}]$ near the critical regime of the M-I transition is observed in conducting polymers over a wide range of temperatures, unlike in other systems.[1(b)] On the metallic side of the

M-I transition, the localization-interaction model provides a good description of the transport properties. In the insulating regime, the $\ln \sigma \propto T^{-x}$ dependence indicates variable-range-hopping (VRH) conduction. The disorder in ''metallic'' polymers arises from a combination of the sample preparation (polymerization), the processing conditions, and the doping procedures; by varying the conditions, one can to some extent control the disorder.

Even within the same batch of carefully prepared samples, the transport properties show some sample-to-sample variation as a result of slight differences in the disorder. In order to avoid this additional complication, one can study the M-I transition in a single sample by progressively aging the sample and following the transport from the metallic regime to the insulating side. Earlier Kaneko and Ishiguro[2] attempted such an experimental study of $FeCl_3$-doped $(CH)_x$ samples. Sulfuric acid doped PPV (PPV-H_2SO_4) is a much better system for such a study, because the dedoping process in this system is nearly reversible. In fact, the yellowish-orange color of pristine samples is fully recovered after dedoping the previously doped, black samples. Thus the main focus of this work is to investigate the transport properties on individual samples from the metallic state to the insulating state by gradually aging the sample during dedoping. In this way, the extrinsic contributions form sample-to-sample variations in structural disorder are avoided.

In a previous publication,[3] we reported the transport properties in the metallic state of PPV-H_2SO_4. For tensile drawn samples with draw ratio of 10, $\sigma_{\parallel}(300\ \mathrm{K}) \cong 10\,000$ S/cm and $\sigma_{\perp}$ (300 K)$\cong$100 S/cm, and the resistivity ratio $[(\rho_r \sim \rho(1.3\ \mathrm{K})/\rho(200\ \mathrm{K})]$ is as low as 1.1. A positive TCR was observed in some samples below 20 K. The sign and magnitude of the magnetoconductance (MC) were found to be dependent on the angle between the chain and field directions. The MC has a strong positive component when the field is perpendicular to the chain axis (transverse MC), whereas the positive component is negligible when the field is parallel to the chain orientation. Such strong anisotropy in MC is consistent with that previously observed in tensile-drawn (stretch-oriented) $(Ch)_x$ samples doped with iodine.[4] The relatively large zero-temperature conductivity, the sign of the TCR at low temperatures, and the sign and magnitude of the anisotropic MC in PPV-H_2SO_4 are all consistent with transport dominated by contributions from weak localization (WL) and electron-electron (e-e) interactions in a disordered anisotropic metal.

We have extended the transport measurements on PPV-H_2SO_4 samples to the critical and insulating regimes. The conductivity and MC are studied in all the three regimes (metallic, critical and insulting) by aging doped samples; the complete M-I transition was monitored in a single sample by controlled aging. We present the conductivity and MC results as a function of ρ_r, which serves as qualitative measure of the carrier concentration and the extent of disorder. In the metallic state, the TCR changes sign from positive to negative at $\rho_r \cong 1.2$.We have observed a magnetic-field-driven transition from metal to insulator via the critical regime. The positive MC vanishes at the M-I boundary. The resistivity follows a power law near the critical regime, and exhibits variable-range hopping in the insulating regime. The large negative MC in the insulating state is also typical of that observed for hopping transport. The $\sigma(T)$ and MC are qualitatively similar for transport parallel and perpendicular to chain axis, suggesting that oriented conducting polymers are anisotropic 3D systems as a result of relatively strong interchain interactions.

II. EXPERIMENTAL DETAILS

The synthesis of PPV and other experimental procedures were described in an earlier publication.[3] For transport measurements in directions parallel and perpendicular to the chain axis, samples were cut parallel and perpendicular, respectively, to the draw direction. Conductivity and MC measurements were carried out in a low-temperature cryostat equipped with a superconducting magnet, enabling measurements from room temperature to 1.3 K in magnetic field from zero to 8 T. The MC measurements were carried out with the field perpendicular to the chain orientation.

The conductivity measurements were monitored *in situ* during doping to optimize the doping level and to achieve maximum conductivity. After each low-temperature transport run, the sample probe was removed for the cryostat and exposed to ambient atmosphere for a specific period. Although the chemistry of the aging process is not well understood, it seems that minute amounts of moisture and oxygen are sufficient to dedope the sample and lower the conductivity. During the aging process the conductivity was continuously monitored. Once the desired conductivity was reached, the sample was quickly inserted into the cryostat where the aging process was stopped by rapid cooling to temperatures below 250 K. Low-temperature transport measurements were carried out after each aging step.

Most of the work was carried out with a single sample. This fresh, fully doped, parallel cut sample is labeled as A $[\sigma(200\ \mathrm{K}) \cong 8670$ S/cm]. Successive low-temperature runs on this sample after each aging step are labeled in alphabetical order from B (8490 S/cm) to I (280 S/cm); eight steps in total. Since this sample failed after the eighth aging step (I), a newly aged sample (J) from the same batch (essentially identical to the sample in run A) was used for carrying out the low-temperature runs deep on the insulating side. After maximum doping, sample J was aged so that its conductivity at 200 K was 82 S/cm; i.e., lower than that of sample I. After this aging step (from maximum conductivity to sample J), this sample was further aged in two steps for runs K and L $[\sigma(200\ \mathrm{K}) \cong 1.2$ S/cm]. One perpendicular cut sample ($M_1^{\perp}$A, labeled $M_1^{\perp}$ in Ref. 3) from the same batch was also measured (aged sample $M_1^{\perp}$B).

III. RESULTS AND DISCUSSION

A. Classification of the metallic, critical, and insulating regimes

Although it is well known that finite conductivity as $T \rightarrow 0$ K is the fundamental definition of the metallic state, extrapolation of $\sigma(T)$ from temperatures above 1 K to sub-Kelvin temperatures is not a straightforward procedure, especially when the system is near the M-I boundary.[1(b)] Thus the extrapolation from $\sigma(T)$ vs T plots may not be adequate to identify the various regimes near the M-I transition (es-

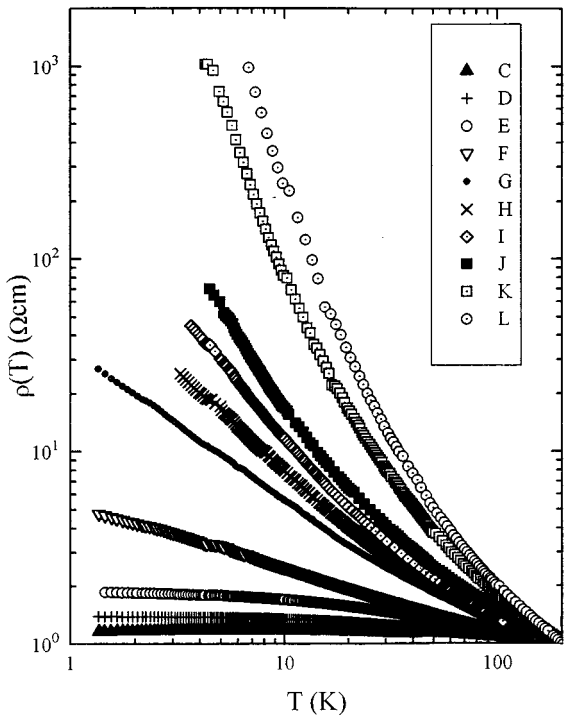

FIG. 1. Resistivity vs temperature of runs C–L. For data on these runs, see Table I.

pecially the critical regime). In order to describe the characteristic behavior of $\rho(T)$ or $\sigma(T)$, explicitly, we define the reduced activation energy W as the logarithmic derivative of $\rho(T)$,[5]

$$W=-T\{d\ \ln\rho(T)/dT\}=-d(\ln\rho)/d(\ln T)=d(\ln\sigma)/d(\ln T). \tag{1}$$

The temperature dependences of W in various regimes are as follows: (a) In the metallic state, W has a positive temperature coefficient. (b) In the critical regime, W is temperature independent for a wide range of temperatures. (c) In the insulating state, W has a negative temperature coefficient. In the disordered metallic regime, the low-temperature conductivity is determined by contributions from weak localization and e-e interactions as described below. In the critical regime of the M-I transition, the correlation length is large and has a power-law dependence on $\delta=|E_F-E_c/E_F|<1$ with critical exponent ν, $L_c=a\,\delta^{-1/\nu}$, where a is a microscopic length, E_F is the Fermi energy and E_c is the mobility edge.[6] In this critical region,[7] the resistivity is not activated, but rather follows a power-law dependence on the temperature as shown by Larkin an Khmelnitskii,[8]

$$\rho(T)\cong(e^2p_F/\hbar^2)(k_BT/E_F)^{-1/\eta}=T^{-\beta}, \tag{2}$$

where p_F is the Fermi momentum, and e is the electron charge. The predicted range of validity includes $1<\eta<3$; i.e., $0.3<\beta=1/\eta<1$.

In the insulating regime, the resistivity follows the activated temperature dependence characteristic of VRH,[6,9] $\ln\rho\propto(T_0/T)^x$, [i.e., $\rho(T)\propto\exp\{(T_0/T)^x\}$], and the reduced activation energy becomes

$$\log_{10}W(T)=A-x\ \log_{10}T \tag{3}$$

TABLE I. The values for parallel conductivity (with respect to chain direction) $\sigma_0[\sigma(T=0\ \text{K})]$, σ(200 K), and ρ_r for runs A–L; m and m_H for runs in the metallic regime (A–E); β [Eq. (2)] and $T_{\max}$ (upper temperature limit for power-law behavior) for runs in the critical regime; an x and T_0 [Eq. (3)] for runs in the insulating regime. Runs A–I and J–L were done on two different but identical samples. The dotted lines separate the metallic, critical, and insulating regimes.

Sample	σ_0(S/cm)	σ(200 K) (S/cm)	ρ_r	m^*	m_H^*
A	7330	8670	1.18	29	145
B	7170	8490	1.19	−20	57
C	6720	7650	1.16	−120	25
D	4510	6340	1.39	45	143
E	2020	3980	1.87	96	
				β	$T_{\max}$
F	0	2440	4.7	0.34	30
G	0	930	27	0.78	15
				x	T_0
H	0	510	100	0.20	3.3×10^4
I	0	280	390	0.28	2200
J	0	82	750	0.35	700
K	0	12	3×10^5	0.41	610
L	0	1.5	4×10^7	0.49	430

where $A=x\log_{10}T_0+\log_{10}x$. Using Eq. (3), one can determine x from the slope of $\log_{10}W$ vs $\log_{10}T$. In the case of mott's VRH, $x=1/4$, while $x=1/2$ for Efros-Shklovskii hopping.[9] As shown below, the VRH parameters, the value of x and T_0 are determined as accurately as possible from the slopes of the W versus T plots.

The weak temperature dependence of $\rho_\parallel$ vs T for parallel cut, metallic PPV-H_2SO_4 is shown in Fig. 1. Upon dedoping (through aging) the samples (from A to L), the magnitude of $\rho_\parallel(T)$ increases and the temperature dependence becomes stronger. Data characterizing the various stages, such as (extrapolated) zero-temperature conductivity (σ_0), ρ_r, and conductivity at 200 K are presented in Table I. In the five first runs (A–E), we found metallic behavior with a finite zero-temperature conductivity. However, as noted above, such a plot cannot unambiguously identify the various regimes near the M-I transition. The normalized $\rho(T)$ for runs A–E are shown in Fig. 2. The differences between runs A, B, and C in terms of σ_0, σ(200 K), and ρ_r are small. Nevertheless, interesting changes in the low-temperature transport properties were observed; run A has a negative TCR while in runs B and C, the TCR is positive. After run C the aging of the sample was more rapid, as can be seen from the values of ρ_r for runs D, E, etc.

For runs F–I, no finite value for σ_0 was found. Runs F and G exhibit a power-law temperature dependence of conductivity, as expected in the critical regime. The value of the exponent β [see Eq. (2)] are given in Table I. From runs H–L, the data exhibit the typical exponential dependence characteristic of hopping transport in the insulating regime.

Although the data in Figs. 1 and 2 roughly define the division into metallic, critical, and insulating regimes, the ρ vs T plots are not sensitive enough to clearly identify the

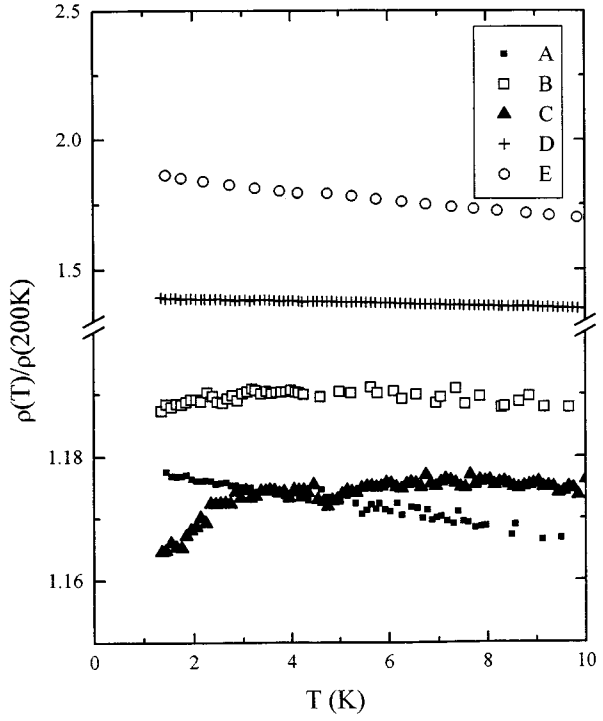

FIG. 2. Normalized temperature dependence of resistivity $\rho(T)/\rho(200\ \mathrm{K})$ vs temperature of runs A–E in the metallic regime.

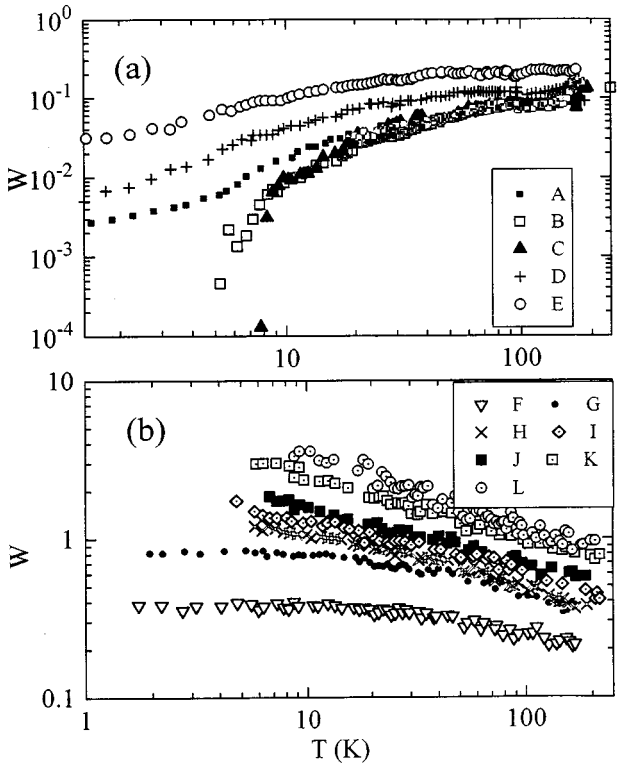

FIG. 3. W vs T for (a) runs A–E on the metallic side and (b) runs E–L on the insulting side of the M-I transition boundary.

boundaries. Thus the same data plotted as W vs T plots are shown in Figs. 3(a) and 3(b). The boundaries of the metallic, critical and insulating regime are quite obvious from the slopes of the W vs T plots: Runs A–E are metallic, F–G are in the critical regime, and runs H–L are insulting. The metallic character of the sample in runs A–E is clearly seen from the positive slope of W at low temperatures. As the M-I transition boundary is approached, the plots exhibit successively smaller slopes. Runs F and G show constant W at low temperatures. This value should equal β as obtained from the low-temperature data of Fig. 1. The two values agree with an accuracy of better than 5%, thus confirming the existence of the power-law behavior. For runs H–L, $W(T)$ indicates variable-range hopping with increasing x. The value of x and T_0 are given in Table I.

B. Conductivity and magnetoconductance in the metallic regime

The analysis of transport data for PPV-H_2SO_4 in the metallic regime was presented in detail in a previous publication;[3] we focus here on features specifically related to the M-I transition. The localization-interaction[10,11] model for disordered metallic systems was found to be consistent with the low-temperature conductivity; $\sigma(T)$ is given by the expression

$$\sigma(T)=\sigma_0+mT^{1/2}+BT^{p/2}, \tag{4}$$

where

$$m=\alpha\left[\tfrac{4}{3}-(3\gamma F_\sigma/2)\right]. \tag{5}$$

The second term ($T^{1/2}$) results from e-e interactions, and the third term is the correction to σ_0 resulting from weak localization; $\alpha=(e^2/\hbar)(1.3/4\pi^2)(k_B/2\hbar D)^{1/2}$ is a function of the diffusion coefficient (D), and γF_σ is the interaction parameter ($\gamma F_J>0$), where $F_\sigma=[\frac{-32}{3}[1-3F/4-(1-F/2)^{3/2}]/F]$, and $F=(1/x)\ln(1+x)$, where $x=(2k_F/K)^2$and K^{-1} is the screening length. Although x diverges near the M-I transition, F varies between 0 and 1. The value of γ depends on the band structure, while p is determined by temperature dependence of the inelastic scattering rate [$\tau^{-1}\propto T^p$] from the dominant dephasing mechanism. Since usually $p>1$, the e-e interaction dominates over weak localization at the lowest temperatures.[10] Thus, below 4 K, the data fit well to a $T^{1/2}$ law. By extrapolating this to zero-temperature, we obtain m and σ_0;these are shown in Table I. In accord with previous results, we obtain best fits for $p=3$, corresponding to electron-phonon scattering.

The $T^{1/2}$ dependence of $\sigma(T)$, observed between 1.3 and 4.2 K, was measured at 0, 5, and 8 T. This is shown in the inset to Fig. 4 for run A (at 0 and 8 T). Although the measured temperature range is not very wide, the $T^{1/2}$ fits are quite satisfactory. Application of a magnetic field causes the TCR to become more negative; that is, the magnetic field increases the magnitude of m. Within the e-e interaction picture, m changes to $m_H=\alpha[(4/3)-\gamma F_\sigma/2]$ when the Zeeman splitting condition ($H/T\gg k_B/g\mu_B=0.7$ T/K) is satisfied. Since γF_σ is always positive, $m_H>m$, in agreement with the observed behavior. In run E [Fig. 4(e)], the MC above 5 T is exclusively negative and, furthermore, the temperature dependence at such fields does not fit the $T^{1/2}$ dependence. This indicates that the sample has crossed into the critical regime. On approaching the M-I transition, m increase, and the positive MC vanishes, as shown in Table I. In Fig. 4, we show the m values as a function of ρ_r. In this

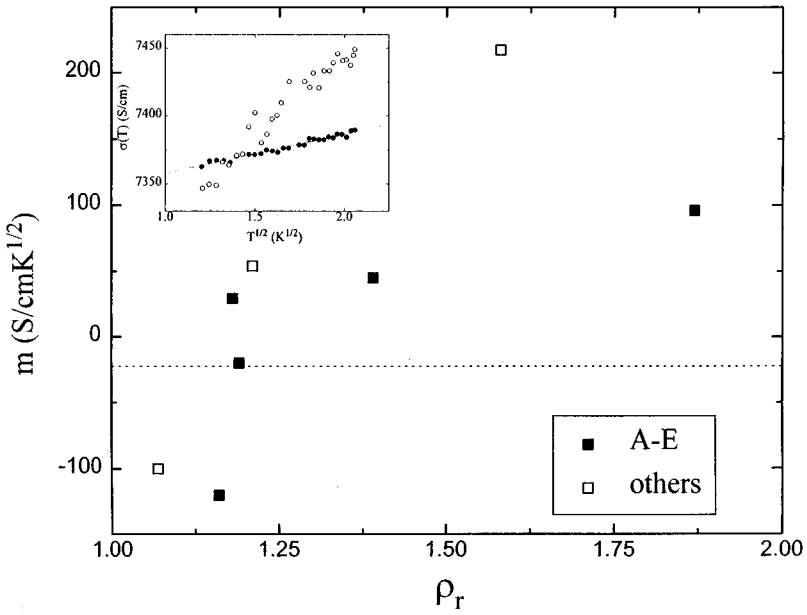

FIG. 4. m vs $\rho_r$in the metallic regime, where m is defined in Eqs. (4) and (5), and $\rho_r=\rho(1.3\ \mathrm{K})/\rho(200\ \mathrm{K})$ is the resistivity ratio. Values are given for a single sample, runs A–E (filled squares),and for other samples (open square). Inset: Conductivity vs $T^{1/2}$ for run A at zero field (●) and 8 T (○).

figure, we have added the m value from other samples that were measured, including those reported in our previous publication.[3] The compiled data point to a crossing from negative values to positive values at $\rho_r \cong 1.2$. Although positive TCR has been observed at low temperature (<20 K) in several conducting polymer systems,[1] only for PPy-PF_6 has a systematic investigation of m vs ρ_r been carried out.[12] In PPy-PF_6, the zero crossing of m was observed at $\rho_r \cong 2$. The

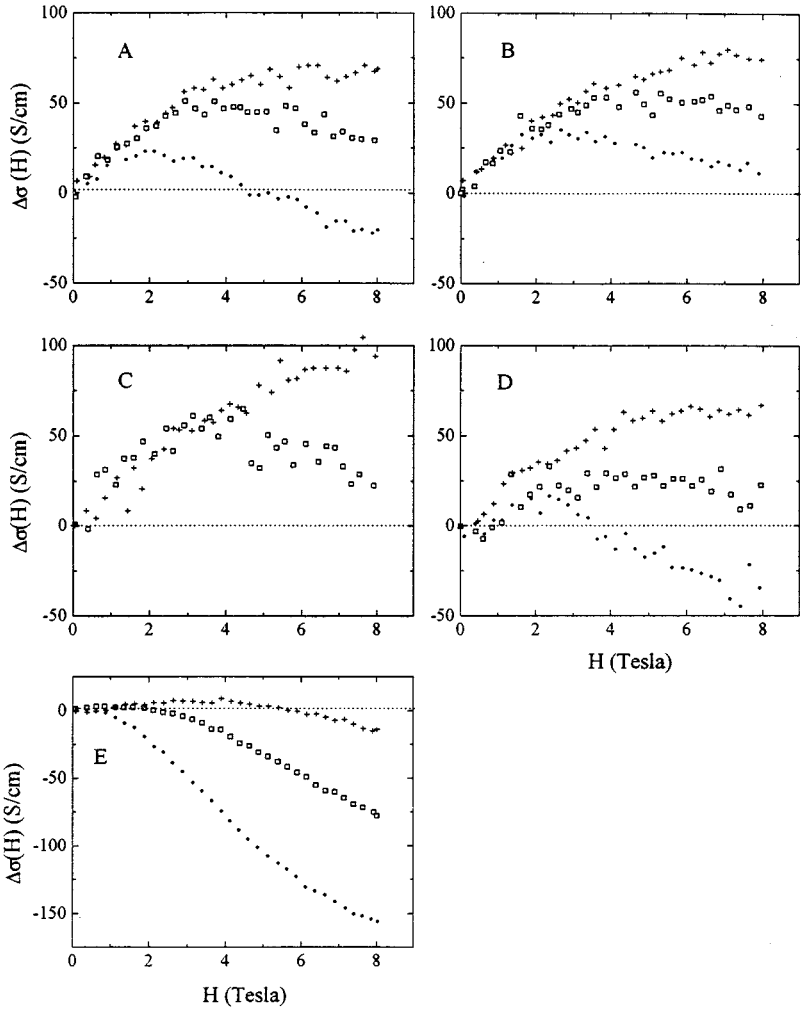

FIG. 5. Magnetoconductance vs field at 1.3 (●), 2.5 (□), and 4.2 K (+) of the same samples A–E as in Fig. 4.

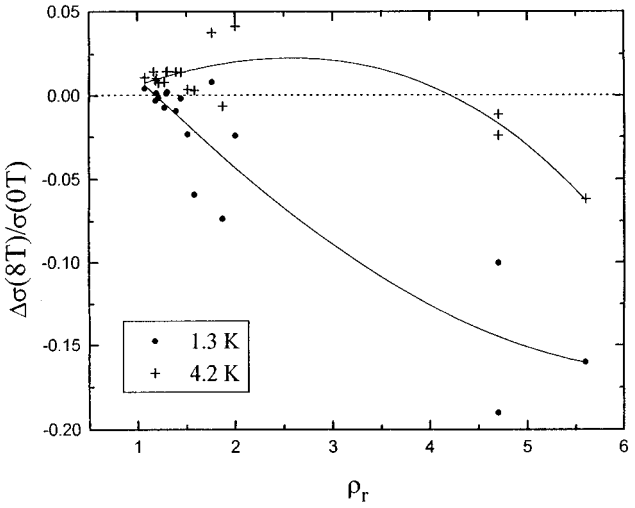

FIG. 6. The normalized magnetoconductance $\Delta\sigma(8\text{ T})/\sigma(0\text{ T})$ vs ρ_r at 1.3 an 4.2 K for different samples, including runs A–F, with $\rho_r<6$. Note the qualitative difference in behavior between 1.3 and 4.2 K. The lines are drawn to guide the eye.

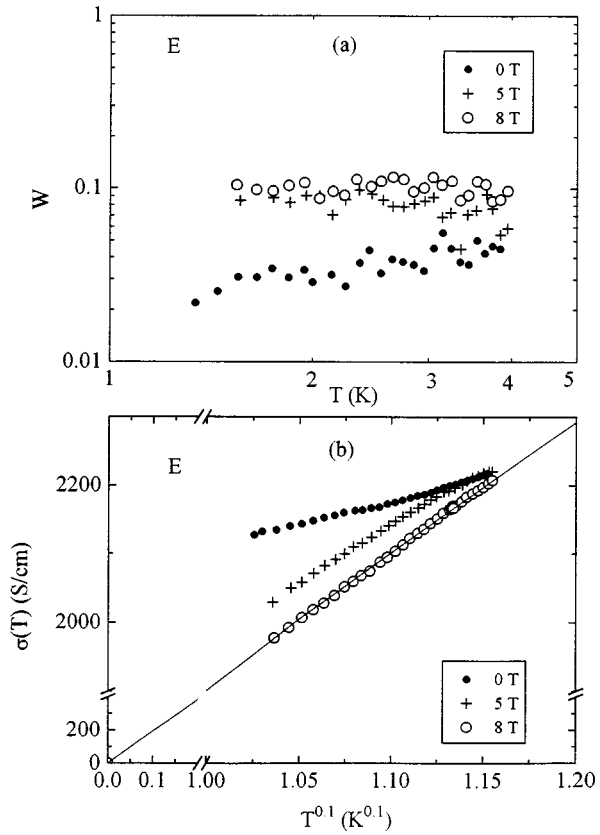

FIG. 7. (a) W vs T for run E at zero field, 5 T and 8 T. (b) Conductivity vs $T^{0.1}$ at the same fields.

sign change of m is well known in the case of heavily doped inorganic semiconductors (Si-P, Si-As, Si-B, Ge-Sb).[11] If F is large (i.e., $\gamma F_\sigma > \frac{8}{9}$), m is negative, and if F is small, m is positive. This might explain the sign change of m near the M-I transition, where screening of the e-e interaction becomes important. For inorganic semiconductors, the dopant concentration can be accurately measured, and the effect of carrier density on the sign and value of m is rather well known. However in conducting polymers this type of work is in its early stages.

The MC data (up to 8 T at 1.3, 2.5, and 4.2 K) for runs A–E are shown in Fig. 5. This is among the first systematic studies of the MC upon aging a single sample from the metallic to the insulating side of the M-I transition. Previously Kaneko *et al.*[13] reported the MC in several samples of iodine doped $(CH)_x$ across the M-I transition. Since MC is a microscopic probe, even slight sample-to-sample variations in structure and morphology could complicate a consistent data analysis. This ambiguity has been avoided by carrying out the MC measurements, from metal to insulator, on a single sample.

For runs A–D, the MC consistently shows a positive contribution at low fields; at higher field, the negative contribution to MC starts to dominate. This is consistent with the field dependence of $\rho(T)$. The WL (e-e interaction) contribution dominated at higher (lower) temperatures and lower (higher) fields. This similarity in behavior is expected since the value of ρ_r for runs A ($\rho_r \cong 1.18$) to D ($\rho_r \cong 1.39$) are rather close. Quantitative analysis of the WL and e-e interaction contributions to the MC in the metallic regime is represented in Ref. 3. We briefly summarize this analysis. At low fields, the H^2 dependence of the MC is dominated by the WL contribution. Although the MC results principally from e-e interaction at high fields ($H^{1/2}$ dependence), WL must still be taken into account in a quantitative analysis. The e-e interaction contribution to the high-field MC is proportional to $(m_H - m)$, which is obtained from the temperature dependence of the conductivity, $\sigma(T) = \sigma(T) = mT^{1/2}$. The WL contribution can be subtracted from the low-field MC since it is nearly temperature independent, providing an alternative way to estimate the e-e interaction contribution. The results obtained from the two methods are consistent, showing the validity of our interpretation of the data. The field at which the MC reaches maximum ($H_{\max}$) increases with increasing temperature. The ratio ($H_{\max}/T$) at 1.3 and 2.5 K is approximately constant in each case with strong positive MC, this being an indication of the Zeeman splitting condition ($H/T \gg 0.7$ T/K). For runs A–D, this ratio varied from 1.4 to 1.9 (larger than 0.7 T/K), in accord with previous results.[3]

We show here, systematically, how the features described above change as the system moves into the insulating regime. Once again, the data indicate that the positive and negative contributions to the MC result from the interplay between the WL and e-e interaction contributions, respectively. When ρ_r increases to 1.87, run E, the positive contribution from WL becomes considerably weaker, as shown in Fig. 5. Also, the $H_{\max}/T$ ratio moves to lower values. Although the W vs T plot for this sample (see Fig. 3) shows a metallic positive temperature coefficient, the absence of a large positive MC (as expected for weakly disordered metallic systems) implies that run E is just on the metallic side of the M-I transition. Thus the vanishing of positive MC can be considered as a sensitive indicator of the approach to the M-I transition boundary from the metallic side. Moreover, the total MC at low field is near zero as a result of the cancellation of positive (WL) and negative (e-e interactions) contributions (as in run E), another important characteristic

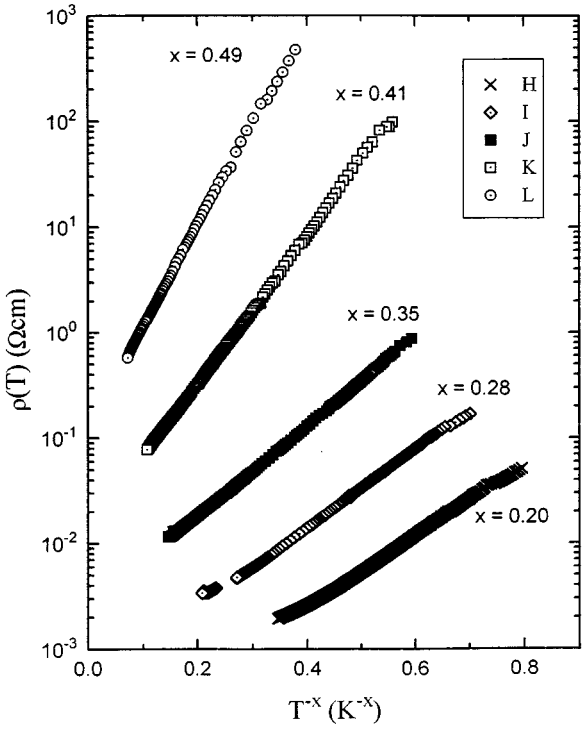

FIG. 8. Resistivity vs T^{-x} for runs H–L in the insulating regime. x is defined in Eq. (3).

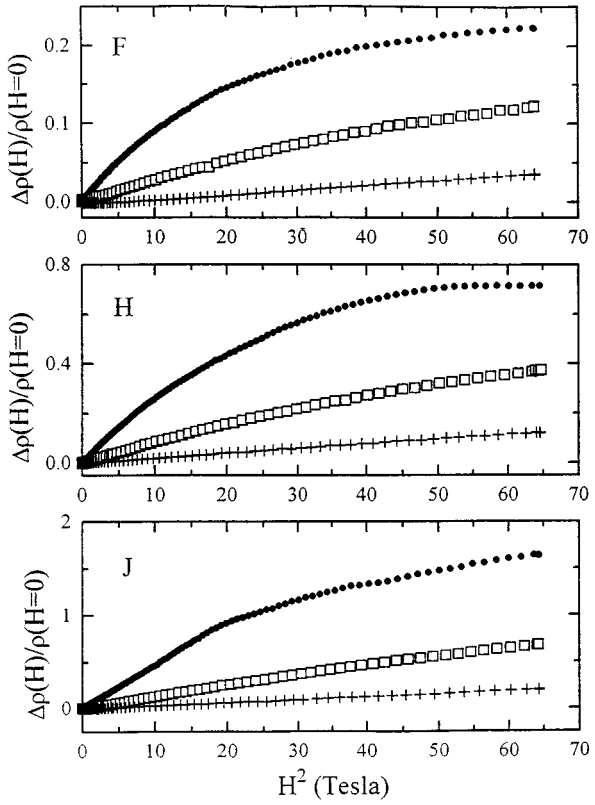

FIG. 9. Normalized magnetoresistance $\Delta\rho(H)/\rho(H=0)$ vs H^2 for runs F, H, and J at 1.3 (●), 2.5 (□),and 4.2 K(+).

of the approach to the M-I transition. The qualitative features of the MC (and their interpretation) for PPV-H_2SO_4 are similar to those observed for Si-P, although the relative magnitude of the positive MC effect is considerably larger in the polymer. In Si-P, the most thoroughly studied system near the M-I transition,the positive MC due to WL was observed only for samples well inside the metallic regime; for those closer to the boundary, the MC is negative.[14]

The $\Delta\sigma(8\text{ T})/\sigma(0\text{ T})$ vs ρ_r plot for $\rho_r \leqslant 6$, is shown in Fig. 6. Positive values for $\Delta\sigma(8\text{ T})/\sigma(0\text{ T})$ are observed at 4.2 K and $\rho_r \leqslant 2$. Furthermore, a maximum seems to exist close to $\rho_r = 2$. At lower temperature, $\Delta\sigma(8\text{ T})/\sigma(0\text{ T})$ tends to more negative values. At 1.3 K, the sign of $\Delta\sigma(8\text{ T})/\sigma(0\text{ T})$ is mainly negative, and its magnitude increases as ρ_r increases. As the disorder increases ($\rho_r > 2$), the increasing (negative) magnitude of $\Delta\sigma(8\text{ T})/\sigma(0\text{ T})$, 5% or more, indicates that transport among localized states starts to dominate, as in Fig. 6. This is consistent with observations in aged $(CH)_x$ samples doped with iodine.[13]

C. Tuning from the metallic to the critical regime with magnetic field

The M-I transition in conducting polymers is very interesting in comparison with other systems because, in the critical regime, $\rho(T)$ follows a power-law temperature dependence over a wide range of temperatures. The critical regime and the ''tuning'' of the M-I transition by pressure and magnetic field have been studied in detail in several conducting polymer systems. Both a field-induced crossover from the critical to the insulating regime and a pressure-induced crossover from the critical to the metallic regime have ben observed.[1(b),15] A field-induced crossover from the metallic state through the critical regime and into the insulating state has been observed in PPV-H_2SO_4 (run E) having $\rho_r = 1.87$.

The $T^{1/2}$ dependence of $\sigma(T)$ from run E is shown in the W vs T plot of Fig. 7(a). The typical metallic positive temperature coefficient of $W(T)$ at $H=0$ T becomes temperature independent at 5 and 8 T; $\sigma(T)$ follows a power law at high field, as shown in Fig. 7(b). The power law fit $[\sigma(T) \propto T^{0.1}]$ at 8 T in Fig.7(b) is in agreement with the value of $\beta = 0.1$ obtained from the W vs T plot [Fig. 7(a)]. The fit follows a straight line and extrapolates to zero conductivity, thus confirming that the sample is insulating at 8 T. The same effect has been observed in another PPV-H_2SO_4 sample, with $\rho_r = 1.58$ and $\sigma(200\text{ K}) = 6900$ S/cm.

A magnetic-field-induced M-I transition, sometimes called ''magnetic freeze-out,'' has ben reported for doped inorganic semiconductors.[9,16] In these materials, the effect was attributed to the change in the Bohr radius of the dopants caused by the field. The extrapolated zero-temperature conductivity was found to decrease linearly with the field. However, in these magnetic freeze-out effects very near the M-I transition, $\sigma(T) = a + bT^{1/3}$, where $a(H) \rightarrow 0$, when $H \rightarrow 0$; and VRH conduction occurs at very high fields. In the data from run E, the field-induce transition changes the temperature dependence from $T^{1/2}$ (e-e interaction in the disordered metallic regime) to the power law which is expected in the critical regime.

Tuning the critical regime of the M-I transition in conducting polymers by disorder pressure, and magnetic field is of considerable interest, since it enables the exploration of the wave functions at energies near the mobility edge. The

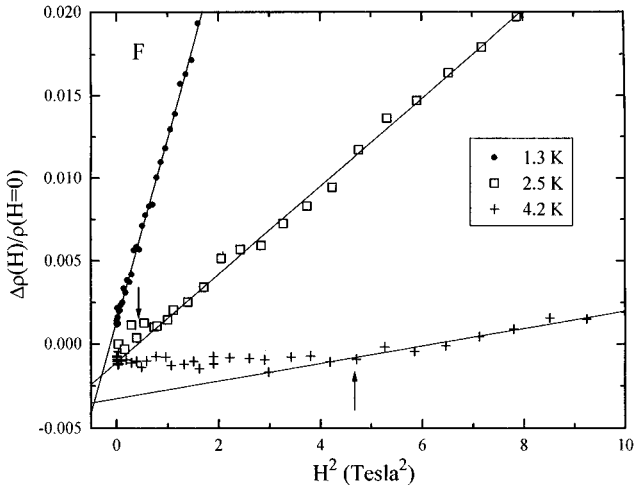

FIG. 10. Normalized magnetoresistance $\Delta\rho(H)/\rho(H=0)$ vs H^2 for run F at low fields. The arrows indicate the field below which there is deviation from H^2 dependence at 2.5 and 4.2 K.

ability to tune through the *M-I* transition from metal to insulator by magnetic field at temperature as high as 10 K suggests that the wave functions near the mobility edge in conducting polymers are more susceptible to localization by the magnetic field than in conventional two- and three-dimensional systems. This could be the result of the quasi-1D character of the electronic structure of conducting polymers and thus to their intrinsic anisotropy.

D. Transport on the insulating side of the *M-I* transition

On the insulating side of the *M-I* transition, the conductivity extrapolates to zero as $T\rightarrow 0$ K. Runs F ($\rho_r\approx 4.7$) and G ($\rho_r\approx 27$) follow a power law [see Eq. (2)] at low temperatures, as shown in Fig. 3(b). The values for the exponent β are within the theoretical estimates, i.e., $\frac{1}{3}<\beta<1$. The exact values of β are shown in Table I. In runs F and G, power-law behavior is observed below 30 ad 15 K, respectively. At lower temperatures in the critical regime (below 1 K), the sample exhibits finite conductivity or not depending on the precise location of the *M-I* boundary. In general, the system is metallic (finite conductivity as T approaches zero) if the value of β is low ($\beta\approx 0.33$–0.5), whereas it behaves like an insulator as $T\rightarrow 0$ if $\beta>0.5$.

The samples in runs H–L show the typical negative temperature coefficient of $W(T)$, as shown in Fig. 3(b). For these sample, $\rho_r>100$, and $\rho(T)\propto\exp\{(T_0/T)^x$ at low temperatures. The values of x and T_0, obtained directly from the W vs T plots [Fig. 3(b)], are summarized in Table I. The exponential fits to the data from runs H–L, using the values of x obtained from W vs T plots, are quite satisfactory, as shown in Fig. 8.

As the system moves to the insulating regime, the negative magnetoresistant (MR) (positive MC) vanishes and the positive MR increases dramatically. This large positive MR in the insulating regime is mainly due to the reduction of the overlap of the localized wave functions in the presence of a field and its effect on the hopping transport among the localized states. The general expression for the MR at low fields in systems showing VRH is given by[9]

$$\ln(\rho(H)/\rho(0))=t(L_c/\lambda)^4(T_0/T)^{3x}H^2, \qquad (6)$$

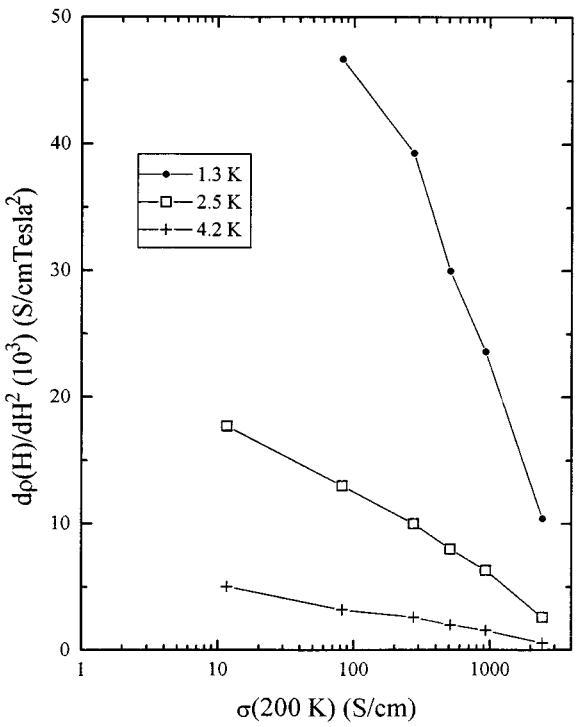

FIG. 11. The low-field magnetoresistance derivative $d\rho(H)/dH^2$ vs $\sigma(200\text{ K})$ for insulating runs F–K at different temperatures (runs F–J at 1.3 K).

where L_c is the localization length, x is the exponent in Eq. (3) and λ the magnetic length. The values for t, for $x=0.25$, and 0.5 are 0.0015 and 0.0035, respectively.

The MR data for runs F, H, and J are shown in Figs. 9(a), 9(b), and 9(c). These figures systematically show that the positive MR increases as the sample becomes more insulating. Qualitatively the behavior of the MR is rather similar in all three cases. This systematic enhancement of positive MR as the system moves deeper into the insulating state is also observed in other conducting polymers.[12,13] The MR is strongly temperature dependent, following an H^2 dependence at low fields, where this H^2 dependence extends to higher fields at higher temperature. At 1.3 K, the MR at higher fields tends to saturate, as expected for hopping transport. At 4.2 K the H^2 dependence is linear up to 8 T. Theoretically, a crossover is predicted from H^2 behavior at low fields to a weaker field dependence at higher fields at a crossover field[9] (H_c)which is proportional to $T^{1/4}$.

The low-field ($H<3$ T) MR of run F is shown in Fig. 10. At 4.2 K, there is hardly any MR at fields up to 2.2 T (marked by the arrow). The MR data in the insulating regime are collected in Fig. 11, which shows the derivative of the MR (with respect to H^2) as a function of conductivity at 4.2, 2.5, and 1.3 K. It is surprising that all the points at a given temperature approximately follow a straight line, even though the conductivities of the different runs vary by several orders of magnitude.

In the zero-field limit, the derivative of Eq. (7) with respect to H^2 is

$$d\ln(\rho(H)/\rho(0))/dH^2=d\rho(H)/dH^2=\text{const}\times T^{-3x}. \qquad (7)$$

In Mott's theory $x=0.75$, while Efros and Shklovskii[9,17] predict $x=1.5$. We have plotted the derivative of all the MR

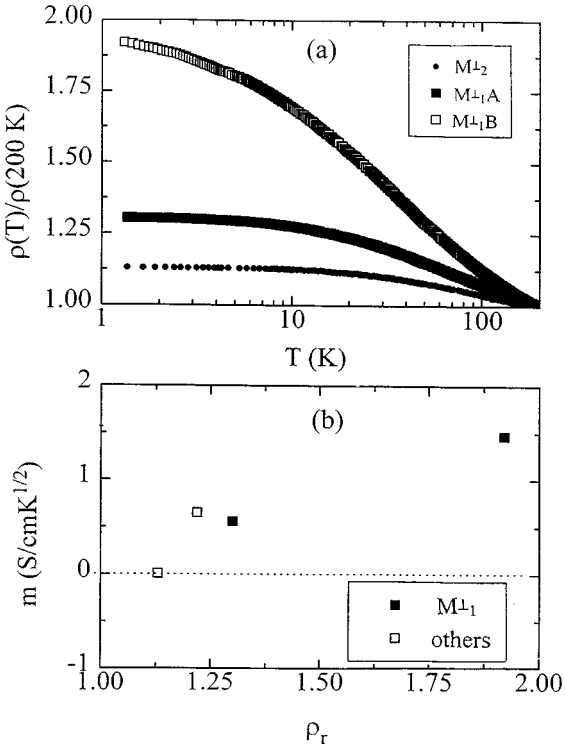

FIG. 12. (a) Normalized temperature dependence of resistivity $\rho(T)/\rho(200\ \mathrm{K})$ vs temperature, perpendicular to the chain direction for sample $M_2^{\perp}$ and $M_1^{\perp}$ as freshly doped (run A) and aged (run B). (b) m vs ρ_r for perpendicular conductivity with respect to chain direction in the metallic regime, where m is defined in Eqs. (4) and (5) and $\rho_r=\rho(1.3\ \mathrm{K})/\rho(200\ \mathrm{K})$ is the resistivity ratio. Values are given for a single sample, $M_1^{\perp}$, runs A and B (filled squares), and for other samples (open squares).

data of insulating samples vs T^{-3x}. In the insulating regime, we found $3x\cong 2\pm 0.2$. Thus the exponent in the MR $(-3x)$ is not in agreement with the exponent of the temperature dependence $(-x)$. This apparent discrepancy is not understood.

E. Conductivity perpendicular to chain axis

In our previous publication on the metallic state in PPV-H_2SO_4 we demonstrated that $\sigma(T)$ and MC behave essentially identically in directions parallel and perpendicular to chain axis.[3] The effect of aging on the transport properties perpendicular to chain has not been studied. Here we briefly summarize the effects of aging on one perpendicular cut sample, and compare the data with results obtained in the direction parallel to chain axis. The freshly doped sample $M_1^{\perp}$ in run A is designated as $M_1^{\perp}$A and, after aging, $M_1^{\perp}$B. $M_2^{\perp}$ is another freshly doped sample from the same batch with draw ratio equal to 10 ($M_1^{\perp}$and $M_2^{\perp}$ were analyzed in Ref. 3). During the aging of sample $M_1^{\perp}$the conductivity at 200 K dropped from an initial value of 120 (run A) to 53 S/cm (run B). The values are shown in Table II. The normalized $\rho(T)$ is shown in Fig. 12(a). The slight difference in the values of ρ_r for samples $M_1^{\perp}$ and $M_2^{\perp}$ is probably due to differences in the doping level. As usual, $\rho(T)$ shows a strong change in T dependence upon aging. The temperature independent resistivity of $M_2^{\perp}$ at low temperatures suggests

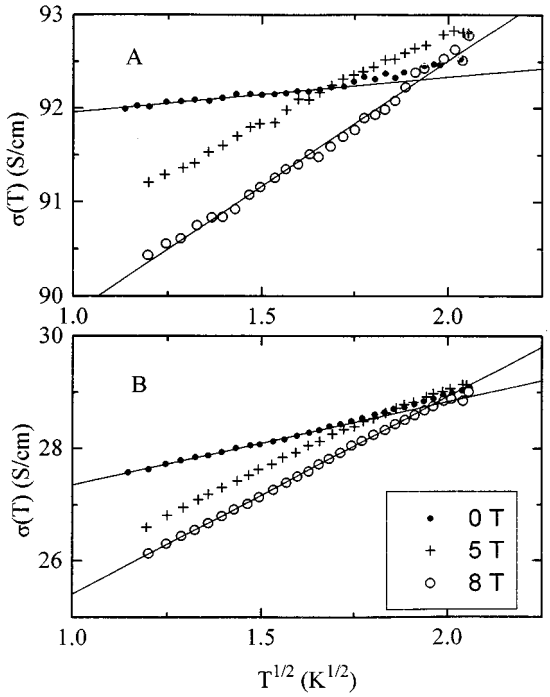

FIG. 13. Conductivity vs $T^{1/2}$ for runs $M_1^{\perp}$A and $M_1^{\perp}$B at zero field (●), 5 T (+), and 8 T (○). The field was perpendicular to the chain axis.

that the charge transport in the direction perpendicular to chain axis is as metallic as in the parallel direction, although the former is nearly two orders of magnitude smaller. This again shows that the system behaves like an anisotropic 3D conductor.

The plot of m vs ρ_r for all the perpendicular cut samples that we have measured is shown in Fig. 12(b). Though there are fewer data points, we conclude that the behavior of m vs ρ_r is similar to that observed in the case of parallel cut samples. Specifically, the zero level crossing of m seems to occur at the same ρ_r value, $\rho_r\cong 1.2$.

The $T^{1/2}$ fit for samples $M_1^{\perp}$A and $M_1^{\perp}$B are shown in Fig. 13. The fit is satisfactory at $H=0$ and at $H=8$ T. The corresponding values of m and m_H are given in Table II.

The MC for runs $M_1^{\perp}$A and $M_1^{\perp}$B are shown in Fig. 14. Once again, as the system approaches the M-I transition, the positive MC becomes weaker, since the WL contribution to the total MC decreases, leaving the e-e interaction contribution to dominate. This is consistent with observations for transport parallel to the orientation axis. The normalized MC at 8 T, $[\Delta\sigma(8T)/\sigma(0T)]$ vs ρ_r is shown in Fig. 15. The behavior is similar to that observed for transport parallel to

TABLE II. The values for perpendicular conductivity (with respect to chain direction) $\sigma_0[\sigma(T=0\ \mathrm{K})]$, $\sigma(200\ \mathrm{K})$, ρ_r, m, and m_H for runs $M_1^{\perp}$A and $M_1^{\perp}$B in the metallic regime. In units of S/cm $\mathrm{K}^{1/2}$.

Sample	σ_0(S/cm)	σ(200 K) S/cm	ρ_r	m^*	m_H^*
$M_1^{\perp}$A	91.6	120	1.30	0.56	2.53
$M_1^{\perp}$B	25.9	53	1.92	1.47	3.50

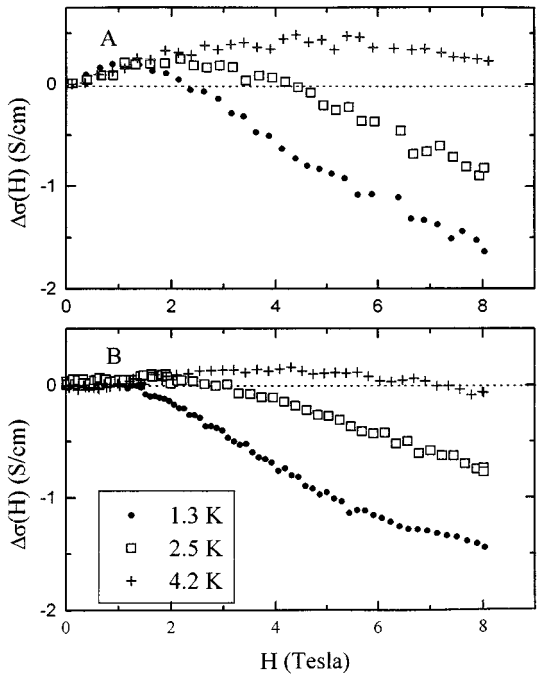

FIG. 14. Magnetoconductance vs field at 1.3 (●), 2.5 K (□), and 4.2 K (+) for the same samples as in Fig. 12(b).

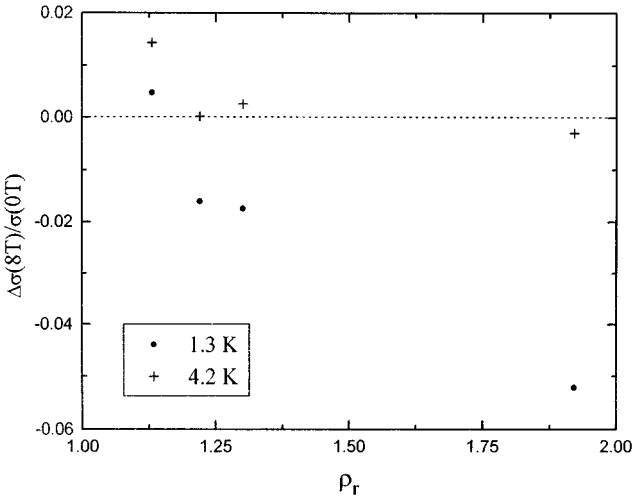

FIG. 15. The normalized magnetoconductance $\Delta\sigma(8\ \mathrm{T})/\sigma(0\ \mathrm{T})$ vs ρ_r at 1.3 and 4.2 K for different perpendicularly cut samples with $\rho_r<2$.

the orientation direction. This again confirms that the microscopic transport mechanisms in parallel and perpendicular directions are nearly identical.

IV. SUMMARY AND CONCLUSION

The temperature dependence of the conductivity and the MC in PPV-H_2SO_4 was studied in detail through the M-I transition. A significant part of this work was carried out on a single sample by aging from the metallic to insulating regime, so that any issues arising from sample to sample variations are ruled out. The main conclusions are the following.

(a) The qualitative behavior of $\sigma(T)$ and MC are similar in directions parallel and perpendicular to the chain axis.

(b) The W vs T plots can easily identify the metallic, critical, and insulating regimes. The transition from metallic to insulating regimes via the critical regime is smooth and continuous.

(c) In the metallic state (runs A–E), the localization-interaction model is satisfactory for explaining both $\sigma(T)$ and MC for directions parallel and perpendicular to the chain axis. The $T^{1/2}$ dependence of $\sigma(T)$ at low temperatures indicates the importance of the e-e interaction contribution. The sign and magnitude of m depends on ρ_r; m changes sign from negative to positive at $\rho_r\cong 1.2$, when moving from the metallic state toward the M-I transition boundary.

(d) The total MC is the sum of contributions from WL (positive MC) and e-e interactions (negative MC). The positive contribution to the MC vanishes as the system approaches the M-I transition, i.e., $\rho_r\cong 2$. The sign and magnitude to the MC depends on ρ_r.

(e) A field-induced transition from the metallic to the critical regime has been observed very near the M-I transition. For the barely metallic sample in run E, $\sigma(T)\propto T^{0.1}$ at 8 T.

(f) The $\sigma(T)$ and MR in the insulting regime (runs H–L) behave in a manner typical of VRH systems. The positive MR increases considerably as ρ_r increases. Just on the insulating side of the M-I transition (run F), the MR is nearly zero at low fields, a cancellation of positive and negative contributions to the MC. This feature vanishes as ρ_r increases in the insulating regime.

(g) The derivative of MR $[d\rho(H)/dH^2]$ in the insulating regime shows a linear trend with $\sigma(200\ \mathrm{K})$, and it is proportional to T^{-2} at low temperatures.

All the results consistently show that oriented conducting polymers of high quality behave as anisotropic three dimensional systems in which the charge transport mechanism is nearly identical in directions parallel and perpendicular to chain axis.

In the critical regime of the M-I transition, power-law behavior has been observed for $\sigma(T)$, $\sigma(T)=aT^b$, over an unusually wide temperature range. The broad temperature range over which the power law is observed, and the ability to tune through the transition by controlling the disorder (as quantified by the resistivity ratio), and by applying external pressure or magnetic fields are special features, not typically observed in disordered inorganic semiconductors, to our knowledge. Although the transport and magnetotransport data imply that conducting polymers are three-dimensional conductors, the high anisotropy of oriented samples implies that the quasi-one-dimensional nature of the conducting polymer chains plays an important role. Unfortunately, however, a detailed theoretical description of the metal-insulator transition in highly anisotropic (quasi-one-dimensional) con--ductors is not available.

ACKNOWLEDGMENTS

This research was supported by the Materials Research Laboratory Program of the National Science Foundation under Award No. DMR-9123048. M. A. thanks the Neste Oy Foundation (Finland) for a personal grant.

[1] (a) Reghu Menon, in *Conductive Organic Molecules and Polymers*, edited by H. S. Nalwa (Wiley, New York, in press); (b) Reghu Menon, C. O. Yoon, D. Moses, and A. J. Heeger, in Metal-Insulator Transition in *Handbook of Conducting Polymers*, 2nd ed., edited by T. A. Skotheim, R. L. Elsenbaumer, and J. R. Reynolds (Dekker, New York, 1996); (c) R. S. Kohlman, J. Joo, and A. J. Epstein, in *Physical Properties of Polymers Handbook*, edited by J. Mark (AIP, New York, 1996).

[2] H. Kaneko and T. Ishiguro, Synth. Met. **65**, 141 (1994).

[3] M. Shlskog, Reghu Menon, A. J. Heeger, and T. Ohnishi, Phys. Rev. B **53**, 15 529 (1996).

[4] Reghu Menon, K. Väkiparta, Y. Cao, and D. Moses, Phys. Rev. B **49**, 16 162 (1994).

[5] A. G. Zabrodskiĭ and K. N. Zinovjeva, Zh. Eksp. Teor. Fiz. **86**, 727 (1984) [Sov. Phys. JETP **59**, 425 (1984)].

[6] N .S. Mott and E. A. Davis, *Electronic Processes in Non-Crystalline Materials* (Clarendon, Oxford, 1979).

[7] W. L. McMillan, Phys. Rev. B **24**, 2739 (1981).

[8] A. I. Larkin and D. E. Khmelnitskii, Zh. Eksp. Teor. Fiz. **83**, 1140 (1982) [Sov. Phys. JETP **56**, 647 (1982)].

[9] B. I. Shklovskii and A. L. Efros, *Electronic Properties of Doped Semiconductors* (Springer-Verlag, Berlin, 1984).

[10] P. A. Lee and T. V. Ramakrishnan, Rev. Mod. Phys. **57**, 287 (1985).

[11] P. Dai, Y. Zhang, and M. P. Sarachik, Phys. Rev. B **45**, 3984 (1992), and references therein.

[12] C. O. Yoon, Reghu Menon, D. Moses, and A. J. Heeger, Phys. Rev. B **49**, 10 851 (1994).

[13] H. Knaeko, T. Ishiguro, J. Tsukamoto, and A. Takahashi, J. Phys. Soc. Jpn. **62**, 3621 (1993).

[14] T. F. Rosenbaum, R. F. Milligan, G. A. Thomas, P. A. Lee, T. V. Ramakrishnan, and R. N. Bhatt, Phys. Rev. Lett. **47**, 1758 (1981).

[15] Reghu Menon, K. Väkiparta, C. O. Yoon, Y. Cao, D. Moses, and A. J. Heeger, Synth. Met. **65**, 167 (1994).

[16] M. C. Maliepaard, M. Pepper, and R. Newbury, Phys. Rev. Lett. **61**, 369 (1988); G. Biskupski, A. El Kaaouachi, and A. Briggs, J. Phys. Condens. Matter **3**, 8417 (1991).

[17] A. N. Ionov and I. S. Shlimak, in *Hopping Transport in Solids*, edited by M. Pollak and B. Shklovskii (North-Holland, Amsterdam, 1991), and references therein.